

Phase Transformation of a Cold Work Tool Steel during Tempering

Hong-xiao CHI^{1,2,3}, Dang-shen MA³, Hui-xia XU², Wang-long ZHU², Jian-qing JIANG¹

(1. School of Materials Science and Engineering, Southeast University, Nanjing 211189, Jiangsu, China;

2. Jiangsu Engineering Research Center of Tool and Die Steel, Tiangong Group, Danyang 212312, Jiangsu,

China; 3. Institute for Special Steels, Central Iron and Steel Research Institute, Beijing 100081, China)

Abstract: The hardness and microstructure evolution of a 8% Cr cold work tool steel during tempering for 40 h were investigated. Transmission electron microscope examinations showed that M_3C carbides precipitated from supersaturated martensite after tempering at 350 °C. When the tempering temperature was higher than 520 °C, the $M_{23}C_6$ carbides precipitated to substitute for M_3C carbides. After ageing at the temperature of 520 °C for 40 h, it was observed that very fine and dense secondary Mo_2C precipitates were precipitated. Thus, it can be concluded that the early stage of Mo_2C -carbide precipitation is like to be Guinier-Preston (G-P) zone formed by [Mo-C] segregation group which is responsible for the secondary hardening peak at 520 °C. Overageing at 700 °C resulted in recovery of martensitic microstructure and precipitation of $M_{23}C_6$ carbides. When ageing at 700 °C for more than 20 h, recrystallization occurred, which resulted in a change of the matrix morphology from martensitic plates to equiaxed ferrite. It was noticed that the size of recrystallized grain/subgrain was very fine, which was attributed to the pinning effect of $M_{23}C_6$ precipitates.

Key words: cold work tool steel; secondary hardening; tempering; carbide

Cold work tool (die) steels must possess particularly high hardness and wear resistance to bear very large compressive stress and frictional force. They also need high toughness to avoid break or tipping caused by impact load. The 12% ledeburitic chromium steels, e. g. , AISI D2 and DIN W. Nr. 1.2379 characteristically have a particularly high abrasive wear resistance, due to their high carbon and high chromium contents, but they have only insignificant toughness properties. The 5% chromium steels, e. g. , AISI A2 and DIN W. Nr. 1.2363 have remarkably improved toughness values, but a poorer wear resistance^[1]. In the early 1980s, a new 8% Cr-type cold work tool steel (the typical chemical composition is C 1.0, Cr 8.0, Mo 2.0, Si 1.0 and V 0.25 in mass%) was developed that combined the good wear resistance and compressive strength with the adequate toughness. Due to the excellent comprehensive performance, this type of steels has been widely used in the world^[2,3].

This type of steels is generally used in a quenched and tempered state and, therefore, the precipitation of secondary carbides and the evolution of the matrix

in the steel during tempering determine the properties of the steel. The tempering process usually leads to a decrease in strength due to the precipitation of carbides from carbon that is originally in solid solution in the martensite, especially in high temperature tempering condition. But the 8% Cr-type cold work tool steels have secondary hardening effect. It becomes possible to recover the strength. Many studies about high speed steel showed that depending upon alloy composition and heat treatment, the secondary carbides are usually MC and/or M_2C ^[4-10]. However, to our knowledge, there has been rarely published report on the secondary hardening mechanisms of this type of steels. Recently, Yan et al.^[11] and Djebaili et al.^[12] reported that the secondary carbide which played an important role in 8% Cr-type cold work tool steels (the V content is more than 1%) was MC, but the M_2C carbides were not found. In addition, understanding of the temper softening behavior and phase transformation process during tempering can be useful in improving mechanical performance.

This paper focuses on investigating the secondary

hardening mechanisms, precipitation and phase transformation behaviors of a 8% Cr cold work tool steel during tempering process, for better understanding the characteristic of the steel.

1 Experimental Material and Procedure

The steel was made in small induction furnace melts, and was forged to 12 mm bars. The chemical composition of the material is given in Table 1. All specimens for quenching and tempering were procured in the annealed state, in which the microstructure of the steel consisted of ferrite and spherical carbides.

Table 1 Chemical composition of the steel in this investigation

this investigation						mass%
C	Cr	Si	Mo	V	N	Fe
1.0	7.98	1.0	2.0	0.28	0.004	Balance

The specimens were austenitized at 1030 °C for 30 min, air quenched to room temperature and then tempered within the range of temperature between 200 and 650 °C. Some specimens were treated by the standard commercial tempering for 2 h twice at those temperatures. Other specimens were isothermally held at 520 and 700 °C, respectively, for various time of 2, 10, 20 and 40 h, and then air cooled.

Morphology and composition of the carbides were studied by scanning electron microscopy (SEM, S4300), energy dispersive spectroscopy (EDS) and transmission electron microscopy (TEM, H800). Thin foils for TEM were firstly mechanically ground to about 50 μm in thickness and then thinned by a twin-jet polishing facility using a solution of 5 vol. % perchloric acid and 95 vol. % ethanol at -20 °C.

2 Results and Discussion

2.1 Variation of hardness with tempering temperature

The influence of tempering temperature on hardness of the tested steel is shown in Fig. 1. The whole process of hardness change can be described in the following four stages: (1) the hardness firstly decreases as the temperature raises, (2) the hardness begins to increase when tempered at temperature higher than 250 °C, (3) the hardness increases more quickly with tempering temperature higher than 450 °C, and the maximum hardness can be obtained after tempered at 520 °C, and (4) when the tempering temperature exceeds 560 °C, the hardness descends remarkably as the temperature raises. The secondary hardening phenomenon appears at the third stage.

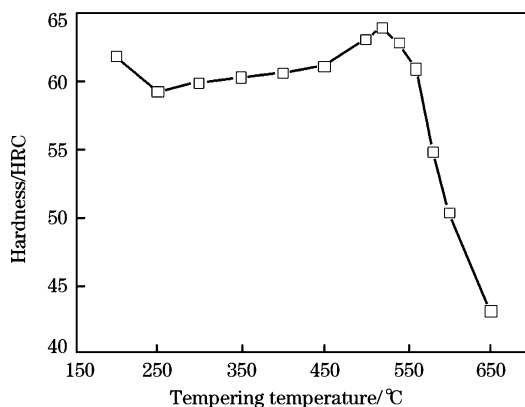


Fig. 1 Relationship between hardness and tempering temperatures

2.2 Phase transformation behavior during the tempering process

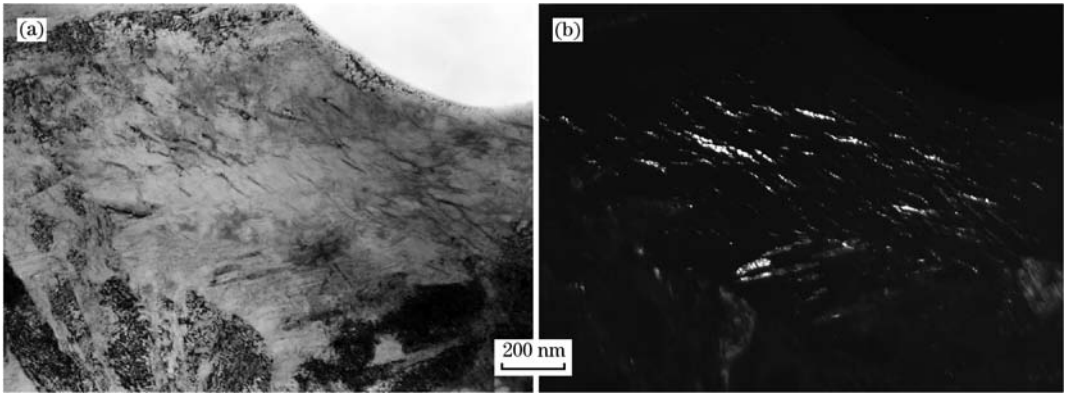
2.2.1 Tempering at 350 °C

Quenched martensite is a supersaturated solid solution of carbon in iron. In the supersaturated solid solution, diffusion effects may bring about the precipitation of new phases along with the hardness decrease of martensite. The types of the precipitated carbide are determined by tempering temperatures. As shown in Fig. 2, a large number of small M_3C carbides were present after the specimen was tempered at 350 °C. It is regrettable that the diffraction pattern was not obtained. But it is almost certain that these carbides are M_3C carbides. In addition, many studies showed that the ϵ carbides were precipitated from matrix during the tempering temperature range of 50 to 250 °C^[13-15]. Yan et al.^[11] also found the ϵ carbides generated in a spray-formed high alloyed steel tempered at 550 °C.

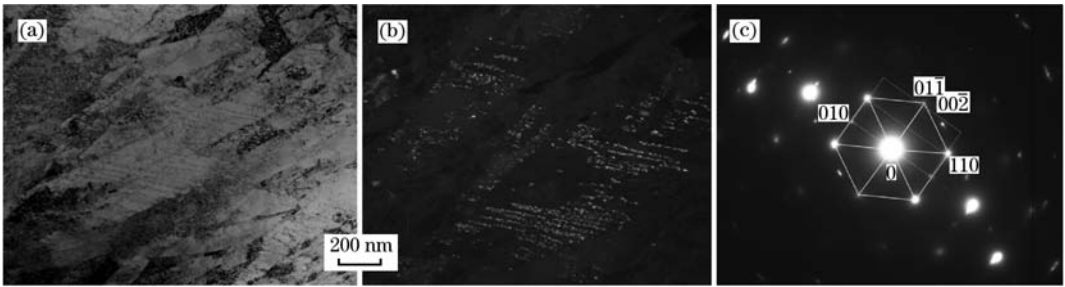
With the precipitation of a large number of M_3C carbides, the carbon content in the matrix becomes lower than before, which weakens the solution strengthening effect. Thus, the hardness gradually decreases as the temperature raises when the tempering temperature is below 250 °C.

2.2.2 Tempering at 520 °C

The peak hardness of secondary hardening appears at 520 °C. However, it is noticed that carbides of both M_2C and MC were not detected during TEM observation. Considering the secondary carbides can precipitate and grow when the steel was aged for longer time. The aging treatment at peak temperature of secondary hardening was carried out on the tested steel. Fig. 3 shows the morphologies of the very fine secondary carbides in the specimens tempered at 520 °C for 40 h. It is observed that the extre-



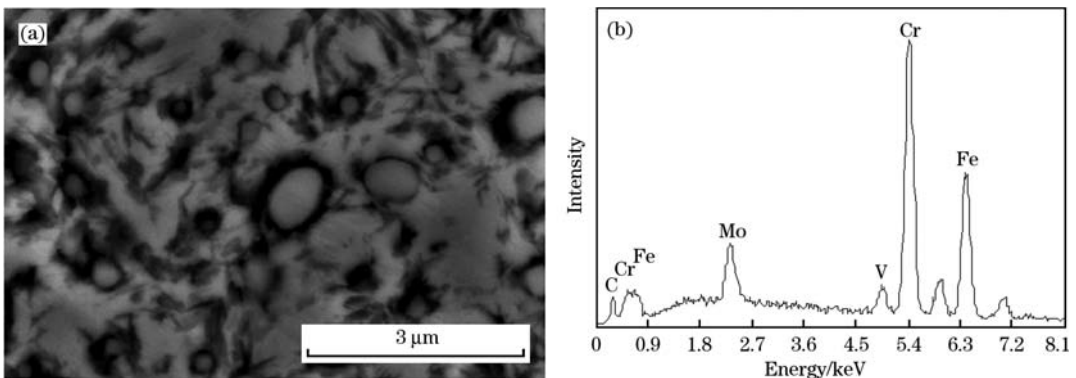
(a) Bright-field image; (b) Dark-field image.

Fig. 2 TEM micrographs showing M_3C precipitates in samples after tempered at $350\text{ }^\circ\text{C}$ **Fig. 3** TEM bright (a) and dark (b) field images of specimen tempered at $520\text{ }^\circ\text{C}$ for 40 h and diffraction pattern (c) of M_2C carbides

mely dispersive fine carbides, with size below 10 nm, are precipitated in the martensite. It is likely that the carbides are precipitated along the dislocation lines in martensite plates as shown in Fig. 3. The fine precipitated carbides in the tested steel are thermodynamically stable and show little tendency to coarsen; even after aging at $520\text{ }^\circ\text{C}$ for 40 h, the size of the carbide remains in the nano-scale. Diffraction patterns as shown in Fig. 3 indicate that the fine precipitates are M_2C (Mo_2C) carbides. However, it should be noticed that carbides in the type of MC ^[11,12] were not detected during this examinations. This is

because the tested steel possesses a lower vanadium content (0.2 mass%); furthermore, the undissolved M_7C_3 and $M_{23}C_6$ carbides contain large amounts of vanadium as shown in Fig. 4. Thus, there is insufficient vanadium providing for the precipitation of VC.

Therefore, it is seen that the extremely fine and dense nature of the dispersive secondary precipitate Mo_2C is the secondary hardening carbide. In fact, it is likely that the early stage of Mo_2C -carbide precipitation, which likes to be Gunier-Preston (G-P) zone formed by $[Mo-C]$ segregation group^[16], is really re-

**Fig. 4** SEM image (a) of specimen tempered at $520\text{ }^\circ\text{C}$ and EDS analysis (b) of carbides

sponsible for the secondary hardening peak at 520 °C.

In addition, it should be noted that the secondary hardening mechanism of the tested steel is the combination of the transformation of retained austenite and the early stage of $M_{23}C_6$ -carbide precipitation, and the role of transformation of retained austenite is more obvious^[17]. The role of transformation of retained austenite on the retard of hardness decrease during tempering process could not be ignored. As can be seen from Fig. 1, the hardness between 250 to 450 °C is gently increased due to the transformation of retained austenite.

2.2.3 Tempering at 700 °C

Above 560 °C, the time to peak hardness and subsequent fall was faster with increasing tempera-

ture. When the tempering temperature was elevated to 700 °C, two obvious changes were observed. Firstly, the martensite in the steel was recovered and started to transform into polygonal ferrite after tempering for 2 h at 700 °C, as shown in Fig. 5(a). It was found that the martensite did not completely decompose when tempered in this condition, and the dislocation density in some areas remains very high. Secondly, a large number of rod-shaped precipitates have been precipitated both along the martensite plate boundaries and within the plates, as shown in the enlarged figure of Fig. 5(a). Most of the precipitates are identified as $M_{23}C_6$ carbides, and the corresponding selected diffraction patterns are shown in Fig. 5(c).

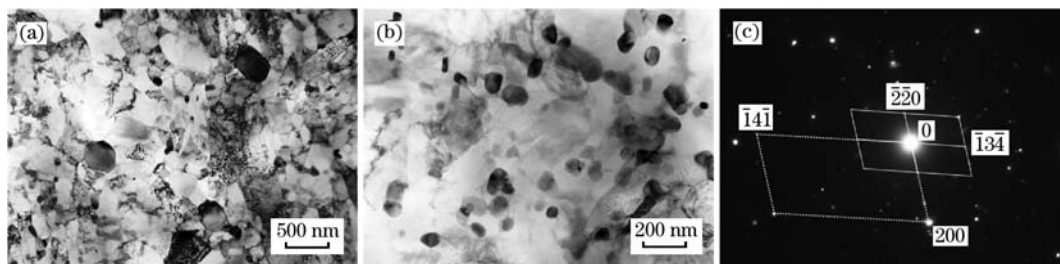


Fig. 5 TEM images of recovery of martensite (a) and $M_{23}C_6$ precipitates (b) of specimen tempered at 700 °C for 2 h and diffraction pattern (c) of $M_{23}C_6$ carbides

It can be concluded that the $M_{23}C_6$ precipitates consist of two parts: (1) a part of $M_{23}C_6$ precipitates were precipitated in the vicinity of M_3C precipitates; (2) the other parts of $M_{23}C_6$ precipitates were directly precipitated from supersaturated bulk martensite. As mentioned above, the M_3C carbides were firstly precipitated from martensite after the steel was tempered at 350 °C. The M_3C carbide precipitation is controlled by carbon diffusion, and the primary rate-controlling element is carbon. According to Shtansky^[18], with the diffusion of carbon, there is also a strong driving force for chromium diffusion towards the surface of cementite particles. With the large amount of chromium in the α' supersaturated solid solution at relatively high temperature, the driving force for cementite precipitation is much reduced. Meanwhile, many investigations show that the solubility of chromium in cementite is limited^[4,19,20]. Thus, it can be concluded that in the tested steel, the amount of chromium in cementite will be saturated with the elevating of temperature. Finally, cementite particles dissolved in the vicinity of alloy carbides, and the $M_{23}C_6$ carbides precipitated instead of cementite with the increase of tempera-

ture. This part of $M_{23}C_6$ carbides are more easy to become bigger due to the short range diffusion and concentration of atoms. The other $M_{23}C_6$ carbides are directly precipitated from supersaturated bulk martensite, which are much finer.

Prolonged tempering at 700 °C for 20 h results in a fully recrystallized, equiaxed ferrite microstructure containing subgrains, with most of the precipitates serving as pinning points for the subgrain boundaries, as shown in Fig. 6. It is noticed that the size of recrystallized grain/subgrain are very fine.

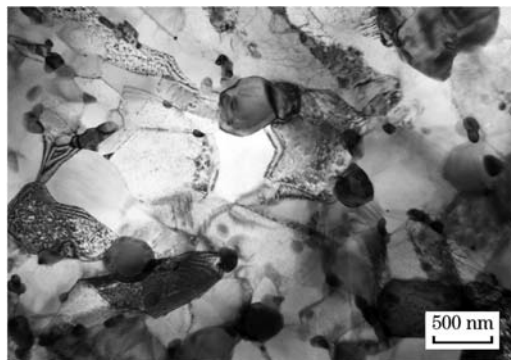


Fig. 6 TEM images of recrystallized grains of the tested steel tempered at 700 °C for 20 h

3 Conclusions

(1) Different types of carbides were precipitated at different tempering temperatures. M_3C carbides were found when the steel was tempered at 350 °C. When increasing the tempering temperature to 700 °C, $M_{23}C_6$ carbides were precipitated in the steel.

(2) It was confirmed by TEM that the very fine and dense nature of secondary M_2C precipitates were precipitated within martensite plates after prolonged tempering for 40 h at 520 °C. The nano-sized M_2C particles are very stable in thermodynamics and show little tendency to coarsen. It can be concluded that the early stage of Mo_2C -carbide precipitation, which likes to be G-P zone formed by [Mo-C] segregation group, is really responsible for the secondary hardening peak at 520 °C for 2 h.

(3) Recovery and recrystallization occurred in 8% Cr type cold work tool steel after tempered at 700 °C. Even after 20 h tempering at 700 °C, the size of recrystallized grain/subgrain was very fine, which was attributed to the pinning effect of $M_{23}C_6$ precipitates.

References:

- [1] F. Jeglitsch, Proceedings of the International Symposium Niobium 2001, Niobium 2001 Ltd., Bridgeville, 2002.
- [2] D. S. Ma, J. H. Liu, Z. Z. Chen, A. J. Kang, H. X. Chi, Iron and Steel 43 (2008) No. 9, 67-70.
- [3] H. X. Chi, D. S. Ma, L. Z. Wu, Z. P. Zhang, Q. L. Yong, J. Iron Steel Res. Int. 17 (2010) No. 6, 43-46.
- [4] K. Kou, J. Iron Steel Inst. 173 (1953) 363-375.
- [5] K. Kou, J. Iron Steel Inst. 174 (1953) 223-228.
- [6] R. Wang, G. L. Dunlop, Acta Metall. 32 (1984) 1591-1599.
- [7] H. F. Fischmeister, S. Karagöz, H. O. Andrén, Acta Metall. 36 (1988) 817-825.
- [8] R. Wang, H. O. Andrén, H. Wisell, G. L. Dunlop, Acta Metall. Mater. 40 (1992) 1727-1738.
- [9] H. Leitner, K. Stiller, H. O. Andrén, F. Danoix, Surf. Interface Anal. 36 (2004) 540-545.
- [10] J. Akré, F. Danoix, H. Leitner, P. Auger, Ultramicroscopy 109 (2009) 518-523.
- [11] F. Yan, H. Shi, J. Fan, Z. Xu, Metall. Charaction 59 (2008) 833-889.
- [12] H. Djebaili, H. Zedira, A. Djelloul, A. Boumaza, Metall. Charaction 60 (2009) 946-952.
- [13] G. R. Speich, K. A. Taylor, Martensite, ASM Int., Ohio, 1992.
- [14] L. Cheng, C. M. Brakman, B. M. Korevaar, E. J. Mittemeijer, Metall. Mater. Trans. A 19 (1988) 2415-2426.
- [15] A. M. Sherman, G. T. Eldis, M. Cohen, Metall. Mater. Trans. A 14 (1983) 995-1005.
- [16] J. R. Chen, C. J. Li, Solid Transformation in Metal and Alloy, Metallurgical Industry Press, Beijing, 1997.
- [17] H. X. Chi, D. S. Ma, C. Wang, Z. Z. Chen, Q. L. Yong, Acta Metall. Sin. 46 (2010) 1181-1185.
- [18] D. V. Shtansky, K. Nakai, Y. Ohmori, Acta Mater. 48 (2000) 969-983.
- [19] J. Janovec, A. Vyrostkova, M. Svoboda, Metall. Mater. Trans. A 25 (1994) 267-275.
- [20] R. K. Shiue, C. Chen, Metall. Mater. Trans. A 23 (1992) 163-170.